Accurate Parameter Estimation of Over-the-Horizon Radar Signals Using RANSAC and MUSIC Algorithms

Igor Djurović[1, *] and Yimin D. Zhang[2]

Abstract—Processing over-the-horizon radar (OTHR) signals is challenging due to appearance of several very close components in the time-frequency plane, strong noise and clutter, multipath propagation, and aliasing. We propose a two-stage procedure for estimating multipath signal components from the received mixture. In the first stage, the instantaneous frequency is estimated from the time-frequency representation of the received signal. The random samples consensus algorithm is applied to the instantaneous frequency estimate to improve the robustness of the procedure against various effects in the underlying signals. In the second stage, the MUSIC algorithm is applied to the dechirped and downsampled signal. The effectiveness of the proposed approach is verified using real-life signals.

1. INTRODUCTION

High-frequency (HF) over-the-horizon radar (OTHR) systems provide effective early warning due to their wide-area surveillance capabilities [1]. The processing of skywave OTHR signals is among the most challenging tasks encountered in applications involving frequency modulated (FM) signals [2–4]. The received signals in the presence of local multipath due to surface reflection near the targets exhibit multi-component Doppler signatures corresponding to different propagation paths toward radar unit [5–9]. These signal components are close to each other in the time-frequency (TF) plane. It is often impossible to visually distinguish such close signal components from their TF representations, which are typically represented as two-dimensional images. Important information about the target geolocation is embedded in the nominal instantaneous frequency (IF) of the signal components and the difference between the individual IFs [10]. Note that the IF may change rapidly within an observation interval as the target maneuvers. Additional processing challenges include the fact that received signals can be heavily cluttered, aliased (when the pulse repetition frequency is below the Nyquist rate), and corrupted by a high level of noise. Addressing such issues related to the OTHR signal processing has practical merits both in this field and also for similar problems encountered in robust processing of rapidly varying FM signals with close components in the TF plane is required.

The basic concept of the two-stage procedure for OTHR parameter estimation is proposed in [9]. In the first stage, the Viterbi algorithm (VA) IF estimator is used to detect the region of the signal components. The complexity of this estimator is high and in the order of $O(N_t N_\omega^2)$, where N_t is number of signal samples and N_ω is the number of frequency bins. The VA is applied to the short-time Fourier transform (STFT) which requires a complexity of $O(N_t N_\omega \log_2 N_\omega)$. In the second stage, close signal components are separated with the high-resolution TF representation referred to as the local polynomial Fourier transform (LPFT). The main problem of this procedure is its high complexity. In that approach, the LPFT results evaluated with various chirp-rate parameters are compared and the

* Corresponding author: Igor Djurović (igordj@ac.me).
[1] Electrical Engineering Department, University of Montenegro, Podgorica 81000, Montenegro. [2] Department of Electrical and Computer Engineering, Temple University, Philadelphia, PA 19122, USA.

output is selected based on a concentration measure of the resulting TF representation. The complexity of the second stage is of $O(N_\alpha N_t N_\omega \log_2 N_\omega)$, where N_α is the number of discretized chirp rates used for the LPFT evaluation. Such high complexity of the existing technique motivates us to develop an alternative algorithm that is able to precisely estimate OTHR parameters but with a substantially reduced computation complexity.

In this paper, as a common practice in this field, we use STFT to evaluate the TF distribution in order to obtain the IF estimate and the region of signal components. A high percentage of the estimated IF entries is corrupted by clutter, noise and other phenomena, and we use the random samples consensus (RANSAC) algorithm [11–13] to improve the IF estimate. The STFT and the RANSAC algorithms produce a coarse estimate of the IF of all received components while in the next stage high-resolution estimation of the close signal components is performed. In the proposed procedure, the received signal is dechirped based on the estimated IF signature from the first stage. Locally, within a short time-interval window, the dechirped signals can be assumed as pseudo-sinusoidal and thus can be estimated using the high-resolution MUSIC algorithm [8] to achieve precise IF estimation of the signal components.

The paper is organized as follows. Section 2 presents the model of the OTHR received signal. The STFT and RANSAC algorithms for the IF estimation and determination of the region of signal components (region-of-interest) are presented in Section 3. Section 4 describes the application of the MUSIC algorithm to the downsampled and dechirped signal for high-resolution IF estimation. Numerical studies validating the proposed technique are given in Section 5, and concluding remarks are presented in Section 6.

2. OTHR SIGNAL

Figure 1 depicts the target and receiver of the OTHR signal based on a flat-earth model [6]. OTHR transmit and receive arrays are typically closely located. For simplicity and without loss generality, we model the OTHR system as a monostatic radar. The OTHR sensor array receives multiple signals from the same target due to multipath propagation with and without earth surface reflection. The combination of the forward and return paths between the transceiver and the target causes four round-trip paths, i.e., I-I, I-II, II-I, and II-II. Because round-trip paths I-II and II-I share the same Doppler signature, the four paths yield three distinct Doppler frequencies in the received signal components which are described as [9]

$$\omega_k(t) \approx \frac{2\omega_c}{c} \left[\left(1 - \frac{2H^2}{R^2(t)} \right) v_R(t) + \frac{2kH}{R(t)} v_c(t) \right], \quad k = -1, 0, 1, \tag{1}$$

where c is the speed of light, ω_c the carrier frequency, H the altitude of the ionospheric layer, and $R(t)$ the ground distance between the target and the radar transceiver. Generally, H is slowly time-varying and thus is assumed to be unchanged during the processing time. The target velocities in the range and ascending directions are $v_R(t) = dR(t)/dt$ and $v_c(t) = dh(t)/dt$, respectively, where $h(t)$ is the target altitude. The difference between the Doppler frequencies of these components reveals important information about the elevation motion velocity of the target, while the IF of the main (middle) Doppler component is associated with the target velocity in the range direction. Since $R(t) \gg H \gg h(t)$ is held, the TF signatures of the received components are close to each other and are difficult to resolve.

3. STFT OF THE OTHR SIGNAL

The baseband signal received by the OTHR unit at the output of array beamforming can be described as

$$x(t) = \sum_{k=-1}^{1} A_k \exp(j\phi_k(t)) = \exp(j\phi_0(t)) \sum_{k=-1}^{1} A_k \exp(j\Delta\phi_k(t)), \tag{2}$$

where A_k is the amplitude of the signal components while $\omega_k(t) = d\phi_k(t)/dt$ is the radian Doppler frequency. The phase difference between the main component ($k = 0$) and the other signal components ($k = 1$ or -1), $\Delta\phi_k(t) \approx 8\pi\omega_c H h(t)/[R(t)c]$, is relatively small since $h(t)/R(t) \ll 1$. Because of the near perfect reflection from the earth surface, the magnitudes A_1 and A_{-1} typically take close values.
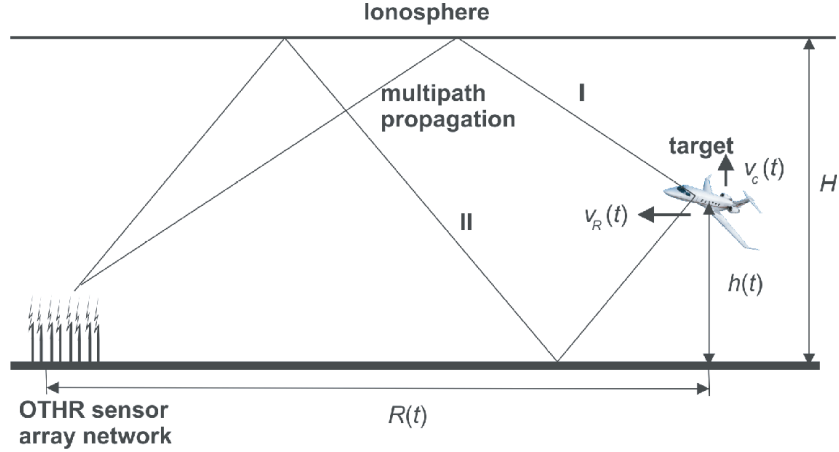
Figure 1. Simplified flat-earth model of the OTHR system.

On the other hand, A_0 corresponds to the combined paths, thus taking a different magnitude. For notational convenience, we denote that $A_1 = A_{-1} = \beta A_0$. Then, the received signal can be described as

$$x(t) = A_0 \exp(j\phi_0(t)) \left[1 + 2\beta \cos(\Delta\phi_k(t))\right]. \tag{3}$$

Therefore, such a signal can be approximated as the FM with amplitude modulation that corresponds to the change of the target altitude. The STFT of the received signal is calculated using a sliding window as

$$STFT(n,\omega) = \sum_k x(t + k\Delta t) w_h(k\Delta t) \exp(-j\omega(k\Delta t)), \tag{4}$$

where Δt is the sampling interval and $w_h(t) = w_h(-t)$ is a symmetric window function of length h, that is,

$$w_h(t) \neq 0 \quad \text{for} \quad |t| < h/2. \tag{5}$$

The position of the TF representation maxima, expressed as

$$\hat{\omega}(t) = \arg\max_\omega |STFT(t,\omega)|, \tag{6}$$

is commonly used as the simplest IF estimator [10]. Due to noise, clutter, amplitude variation and potential aliasing, the IF estimate contains a large percentage of outliers and there may not be a single sample over a relatively wide interval that is close to the signal components. The robust IF estimation method described in [9, 10] exploits the VA [14–17] but this solution is relatively inefficient. The VA IF estimator requires search over all possible paths in the TF plane by minimizing the path penalty function with two criteria, i.e., the IF estimate should pass the TF representation points with a large magnitude, and path variations should be small [14]. Therefore, in this paper, we propose the RANSAC style algorithm to improve the accuracy of the IF estimation [11, 12].

As elaborated in [14] and will be clearly seen from the examples, there are a large number of outliers in the IF estimate obtained from Eq. (6). The percentage of outliers in an interval can be very high, making direct IF estimation challenging.

We model the IF law as a polynomial function:

$$\omega(t) = \sum_{i=0}^{K} a_i t^i. \tag{7}$$

In order to accurately model the complicated OTHR signal, a high-order polynomial signal model is adopted with K being an order of 50 or larger. As such, the IF can be modeled by $K + 1$ samples without outliers. We perform a random selection of the $K + 1$ IF estimate samples:

$$\{\hat{\omega}(t_i) | i \in [0, K]\} \quad \hat{\omega}(t_i) < \hat{\omega}(t_{i+1}). \tag{8}$$

The IF can be re-estimated (effectively filtered) by the polynomial regression of these $K+1$ IF samples, expressed as

$$\hat{\omega}'(t) = \sum_{i=0}^{K} \hat{a}_i t^i, \tag{9}$$

where $\{\hat{a}_i | i \in [0, K]\}$ are the estimated polynomial phase coefficients. In this case, some of the samples in the random selection can be outliers, thereby giving incorrect IF estimates. Therefore, we have to perform multiple random selections and choose the best estimate from the ensembles based on some appropriate criterion. In this paper, we use the RANSAC-based IF (re)estimation, and the developed algorithm is described as follows [11, 12]:

3.1. IF Estimation Algorithm

Calculate the STFT using Eq. (4).
   Obtain the initial IF estimation using Eq. (6).
   For $\lambda = 1 : \Lambda$ (where Λ is maximal number of random selections in the algorithm)
   Perform random selection of samples of IF estimate samples using Eq. (8) and denote them as $\hat{\omega}^\lambda = \{\hat{\omega}^\lambda(t_i) | i \in [0, K+1]\}$ $\hat{\omega}^\lambda(t_i) < \hat{\omega}^\lambda(t_{i+1})$.
   Estimate the coefficients using polynomial regression [18, 19]:

$$\hat{\mathbf{a}}^\lambda = \left(\mathbf{\Gamma}^T\mathbf{\Gamma}\right)^{-1}\mathbf{\Gamma}\hat{\omega}^\lambda, \tag{10}$$

where $\mathbf{\Gamma}$ is a $(K+1) \times (K+1)$ square matrix with elements $\gamma_{ij} = t_i^j$, $i \in [0, K]$, $j \in [0, K]$.
   Re-estimate the IF based on the estimated phase parameters as in Eq. (9):

$$\hat{\omega}^{[\lambda]}(t) = \sum_{i=0}^{K} \hat{a}_i^\lambda t^i. \tag{11}$$

Evaluate the criterion function:

$$J(\lambda) = \text{median}\left[\left|\hat{\omega}_R(t) - \hat{\omega}^{[\lambda]}(t)\right|\right]. \tag{12}$$

End
   Select the best results by minimizing the following criterion function:

$$\hat{\lambda} = \arg\min_\lambda J(\lambda), \tag{13}$$

where the parameters and IF estimates correspond to trial $\hat{\lambda}$ producing the minimal value of the criterion function:

$$\hat{a}_i^f = \hat{a}_i^{\hat{\lambda}}, \quad i \in [0, K], \tag{14}$$

$$\hat{\omega}^f(t) = \hat{\omega}^{[\hat{\lambda}]}(t). \tag{15}$$

In Eq. (12), we used the median of the absolute difference as the criterion in order to minimize the effect of outliers. In addition, we do not compare the reconstructed IF function with the estimate obtained from Eq. (6). Rather, we compare it with the version of the IF function, denoted by $\hat{\omega}_R(t)$, that is a robustly filtered version of $\hat{\omega}(t)$. The robust filtering is applied to avoid comparison of reconstructed IF $\hat{\omega}^{[\lambda]}(t)$ with IF estimate Eq. (6) that can be corrupted by noise, clutter, and aliasing. In this paper, we use the median filter to robustly filter the IF estimate with a relatively long window in order to mitigate the influence of long burst errors in the IF estimation:

$$\hat{\omega}^R(t) = \text{median}\{\hat{\omega}(t + l\Delta t) | l \in [-L/2, L/2]\}. \tag{16}$$

4. FINE ESTIMATION STAGE

In the first stage we estimate the IF that is mainly related to the range-direction motion of the target, $v_R(t)$. Precise estimation of the component $v_c(t)$ is not possible in this coarse estimation stage since the STFT is not a high-resolution TF representation able to separate close signal components. In order to estimate close signal components and the residual errors in estimating $\omega_0(t)$, we first perform the following dechirping:

$$\tilde{x}(t) = x(t) \exp\left(-j\hat{\phi}^f(t)\right) = x(t) \exp\left[-j\sum_{i=1}^{K+1} \hat{a}_{i-1}^f t^i / i\right]. \tag{17}$$

Performing low-pass filtering of this signal reduces the noise and, more importantly, the effect of clutter output in the signal component band:

$$\hat{x}(t) = \text{IFT}\left[\tilde{X}(\omega)H(\omega)\right], \tag{18}$$

where $\tilde{X}(\omega) = \text{FT}[\tilde{x}(t)]$ and $H(\omega) = 1$ for $|\omega| \le \omega_0$ and $H(\omega) = 0$ elsewhere, representing ideal low-pass filtering. After dechirping, signal $\hat{x}(t)$ becomes a three-component FM signal with the following IFs:

$$\Delta\omega_k(t) = \omega_k(t) - \hat{\omega}^f(t), \quad k = -1, 0, 1. \tag{19}$$

Again these three components are close, but the IF variations are substantially reduced and, at least over a short time interval, signal components can be considered stationary. Therefore, we apply a sliding window $x_w(t; \tau) = \hat{x}(t)w_h(\tau - t)$ and, for each interval, a high-resolution spectral estimation technique is applied to obtain a precise IF estimate of the signal components. As one of the best available techniques for this purpose, the root-MUSIC algorithm is utilized [8]. In order to reduce the computational complexity, the root-MUSIC is performed on downsampled signal

$$x_d(t) = x_w(dt), \tag{20}$$

where d is the downsampling factor. The other reason for downsampling is improved visual presentation of the signal components.

There are several important advantages of the proposed technique compared with the high-resolution technique proposed in [9]. First, in the coarse estimation stage we have a precise estimation of the IF while in [9] the computationally demanding VA is used to obtain the IF estimation. The other more important advantage is that the proposed technique does not use the LPFT, which requires a high computation complexity of $O(N_\alpha N_t N_\omega \log_2 N_\omega)$ for the recalculation of the TF representation. Finally, spectral estimators, such as the root-MUSIC, can be directly used to estimate the IF while the LPFT produces only TF images. Note that the LPFT requires the use of some additional algorithms to separate signal components from the TF representation image while in the case of the root-MUSIC algorithm the frequencies of the components follow immediately from the algorithm.

5. EXPERIMENTAL RESULTS

The effectiveness of the proposed technique is validated using real measurement data. The dataset, which consists of return waveforms received from a maneuvering aircraft, was collected by Australian Defence Science and Technology Organisation (DSTO) in April 2003 [8]. During the 181 seconds of observation time, the aircraft makes a 360° turn and, at the same time, it descends the altitude by approximately 2500 meters. The transmit and receive antenna arrays are located on land separated by approximately 100 km. The surface range between the radar site and the target is approximately 1350 km. The carrier frequency is 16 MHz, and the pulse repetition frequency (PRF) is 40 Hz.

Preprocessing using STFT described in Eq. (3) and IF estimation in Eq. (6) is performed after clutter suppression. The computed STFT using the 128-point Hanning window, which amounts to 3.2 s, is depicted in Figure 2(a). Aliasing is observed because the sampling rate is lower than the Nyquist rate. Straightforward antialiasing is performed to correct the position of the aliased region in the TF plane (around 80 s and -20 kHz) to a proper position, yielding a modified STFT as depicted in Figure 2(b). Figure 3 shows the single-trial results when applying the RANSAC algorithm to the

considered signal with polynomial order of $K = 50$. Dashed lines correspond to the positions of the STFT maxima computed using (6), where a large number of outliers are observed. The width of the median filter used for the evaluation of $\hat{\omega}_R(t)$ and the criterion function depicted in (12) is relatively wide 7.5 s. The nine subplots in Figure 3 correspond to the cases when the current minimum of the criterion function $J(\lambda)$ is updated. It is seen that after only 70 trials we obtain an IF estimate without outliers, while after only 87 iterations the value of the cost function $J(\lambda)$ falls below 3500. In our experiment,
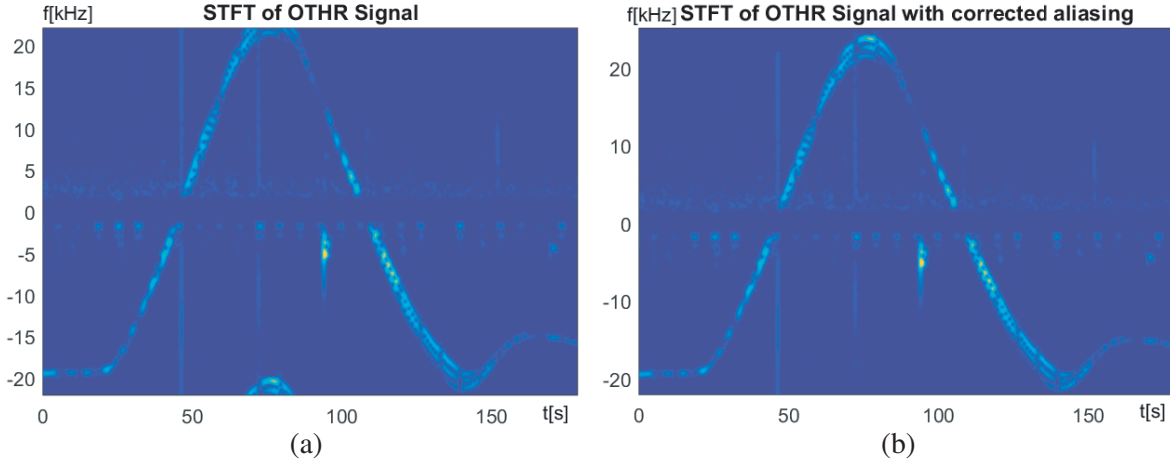

Figure 2. Time-frequency representation of considered signal: (a) STFT of the OTHR signal; (b) STFT with corrected aliasing effect around $t = 80$ s.
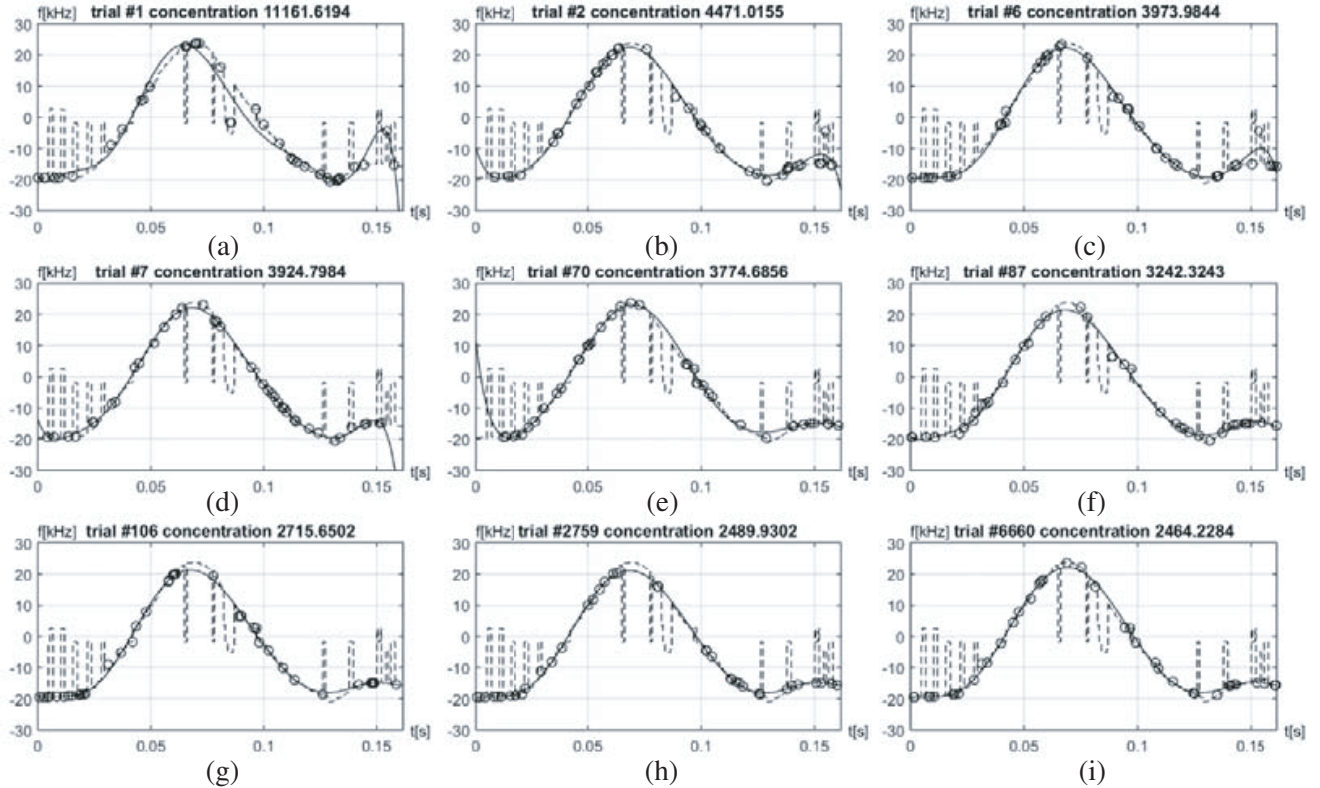

Figure 3. IF estimation of the OTHR signal: Dashed line — position of the STFT maxima; circles — random samples in RANSAC procedure; solid line — IF estimation after polynomial regression of random samples.

we use the value of the cost function $J(\lambda)$ as the indicator of the accuracy of the IF estimation, and the estimated IF results are considered accurate when the value of $J(\lambda)$ is below 3500.

In order to demonstrate the stability of the RANSAC procedure, we repeat the RANSAC for 1000 times. The average, minimal, and maximal values of $J(\lambda)$ are respectively calculated and depicted in
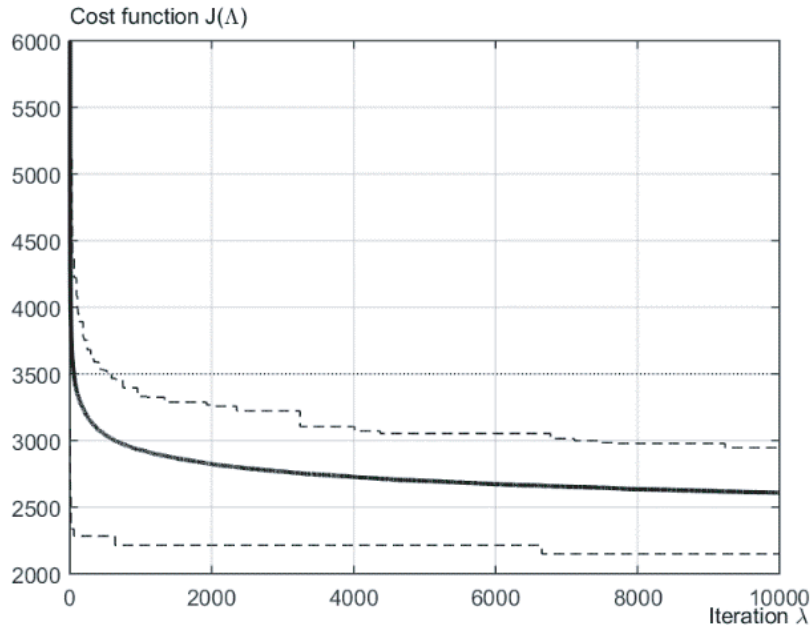

Figure 4. Value of $J(\lambda)$ in 1000 trials: Solid line — average value; dashed lines — minimal and maximal value.
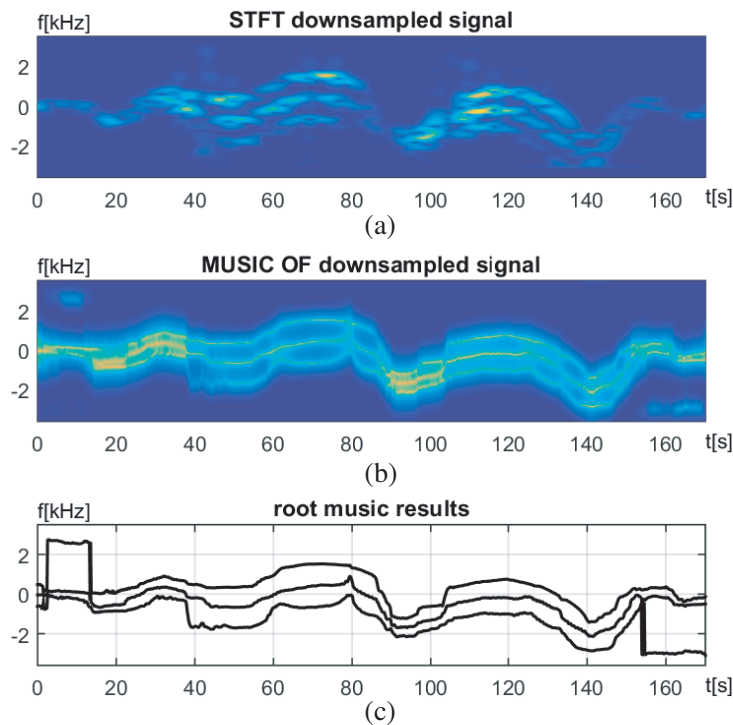

Figure 5. Fine estimation stage: (a) STFT of the downsampled signal; (b) MUSIC pseudo-spectrum of the downsampled signal; (c) Frequencies of the estimated components using root-MUSIC algorithm — lines correspond to estimate IFs.

Figure 4. It can be seen that on average the RANSAC gives the IF estimate without outliers and inaccuracy close to the interval limits for less than 55 iterations ($J(\lambda) < 3500$), while in the worst case (the maximal value of $J(\lambda)$) it gives robust results for less than 450 iterations (in our experiment for 415 iterations). This experiment can help to determine the algorithm setup. The results of the fine estimation stage of the algorithm are shown in Figure 5, where the downsampling factor is $d = 6$. The STFT of dechirped, downsampled, and filtered signal is given in Figure 5(a), while the MUSIC pseudo-spectrum is shown in Figure 5(b). The estimated components using windowed data with 64 samples and the root-MUSIC algorithm are given in Figure 5(c). It verifies the excellent accuracy in estimating signal components that can barely be recognized from the STFT depicted in Figure 5(a). We detect two inaccurate zones at the beginning of interval (around $t = 10\,\mathrm{s}$) and at the end (around $t = 160\,\mathrm{s}$). However, it does not cause errors in the estimated distance between signal components in the TF plane as demonstrated subsequently.

Finally, Figure 6(a) shows the differences in the estimated IF of the close components, $\Delta\omega_{10}(t) = \omega_1(t) - \omega_0(t)$ and $\Delta\omega_{0-1} = \omega_0(t) - \omega_{-1}(t)$, which are associated with the elevation velocity component $v_c(t)$. In order to estimate the difference IF between these close components, we average $\Delta\omega_{10}(t)$ and $\Delta\omega_{0-1}$, $\Delta\omega(t) = [\Delta\omega_{10}(t) + \Delta\omega_{0-1}(t)]/2$. However, if any of $\Delta\omega_{10}(t)$ or $\Delta\omega_{0-1}$ is greater than the predefined threshold of $2\,\mathrm{kHz}$, then we adopt an alternative estimate of the difference between components as $\Delta\omega(t) = \min[\Delta\omega_{10}(t), \Delta\omega_{0-1}(t)]$. The resulting difference between the estimated components is given in Figure 6(b). It is evident that the obtained results are stable, accurate, and free from the influence of any kind of outliers.
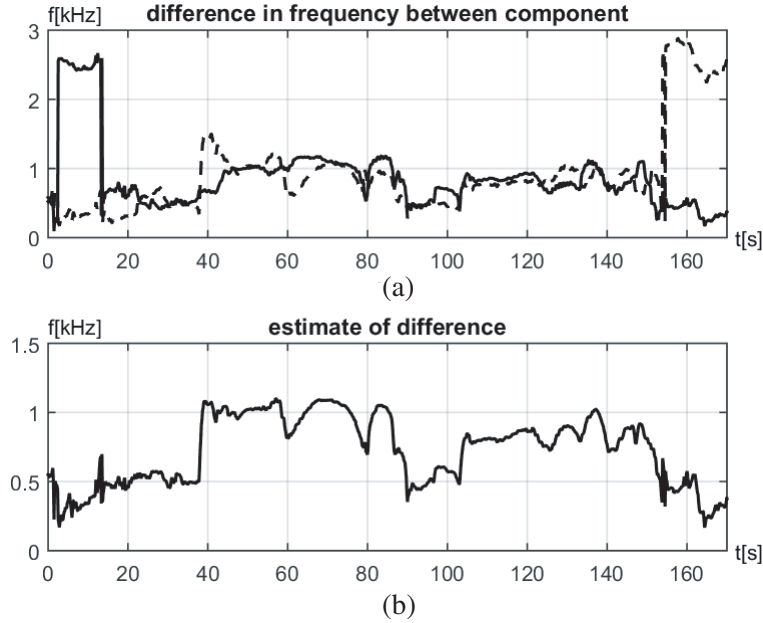

(a)

(b)

Figure 6. Estimation of difference of the IF of signal components: (a) Initial results based on the root-MUSIC algorithm output (solid line is difference $\Delta\omega_{10}(t) = \omega_1(t) - \omega_0(t)$ while dashed line is difference $\Delta\omega_{0-1} = \omega_0(t) - \omega_{-1}(t)$); (b) Result after removing outliers based on the simple thresholding strategy (final estimate $\Delta\omega(t)$).

6. CONCLUSION

In this paper, we have proposed the use of the RANSAC algorithm for the reconstruction of signal parameters in a skywave OTHR system. The RANSAC algorithm is applied to the IF estimate in the coarse estimation stage of the algorithm, which is followed by the root-MUSIC algorithm in the fine estimation stage for the separation of close signal components. The effectiveness of the proposed algorithm is verified using real-life signals.

REFERENCES

1. Fabrizio, G. A., *High Frequency Over-the-Horizon Radar: Fundamental Principles, Signal Processing, and Practical Applications*, Mc-Graw Hill Education, 2013.

2. Lan, H., Y. Liang, Q. Pan, F. Yang, and C. Guan, "An EM algorithm for multipath state estimation in OTHR target tracking," *IEEE Transactions on Signal Processing*, Vol. 62, No. 11, 2814–2826, 2014.

3. Romeo, K., Y. B.-Shalom, and P. Willett, "Detecting low SNR tracks with OTHR using a refraction model," *IEEE Transactions on Aerospace and Electronic Systems*, Vol. 53, No. 6, 3070–3078, Dec. 2017.

4. Thayaparan, T., R. Riddolls, and K. Shimotakahara, "Frequency monitoring system for over-the-horizon radar (OTHR) in Canada," *Proc. of IRS*, May 2016, DOI: 10.1109/IRS.2016.7497370.

5. Headrick, J. and M. Skolnik, "Over-the-horizon radar in the HF band," *Proceedings of the IEEE*, Vol. 62, 664–673, Jun. 1974.

6. Zhang, Y., M. Amin, and G. Frazer, "High-resolution time-frequency distributions for manoeuvring target detection in over-the-horizon radars," *IEE Proceedings Radar, Sonar and Navigation*, Vol. 150, 299–304, Aug. 2003.

7. Wang, G., X.-G. Xia, B. Root, V. Chen, Y. Zhang, and M. Amin, "Manoeuvring target detection in over-the-horizon radar using adaptive clutter rejection and adaptive chirplet transform," *IEE Proceedings Radar, Sonar and Navigation*, Vol. 150, 292–298, Aug. 2003.

8. Ioana, C., Y. Zhang, M. Amin, F. Ahmad, G. Frazer, and B. Himed, "Time-frequency characterization of micro-multipath signals in over-the-horizon radar," *Proc. of Radar Conf.*, May 2012.

9. Djurović, I., S. Djukanović, M. G. Amin, Y. D. Zhang, and B. Himed, "High-resolution time-frequency representations based on the local polynomial Fourier transform for over-the-horizon radars," *Proc. of SPIE*, Vol. 8361, May 2012, doi: 10.1117/12.919954.

10. Stanković, L. J., I. Djurović, S. Stanković, M. Simeunović, and M. Daković, "Instantaneous frequency in time-frequency analysis: Enhanced concepts and performance of estimation algorithms," *Digital Signal Processing*, Vol. 35, 1–13, Dec. 2014.

11. Djurović, I., "A WD-RANSAC instantaneous frequency estimator," *IEEE Signal Processing Letters*, Vol. 23, No. 5, 757–761, May 2016.

12. Djurović, I., "QML-RANSAC: PPS and FM signals estimation in heavy noise environments," *Signal Processing*, Vol, 130, 142–151, Jan. 2017.

13. Sheng, H., Y. Gao, B. Zhu, K. Wang, and X. Liu, "Feature extraction of SAR scattering centers using M-RANSAC and STFRFT-based algorithm," *EURASIP Journal on Advances in Signal Processing*, Vol. 2016, No. 1, 46, 2016.

14. Djurović, I. and L. J. Stanković, "An algorithm for the Wigner distribution based instantaneous frequency estimation in a high noise environment," *Signal Processing*, Vol. 84, 631–643, Mar. 2004.

15. Conru, C., I. Djurovic, C. Ioana, A. Quinquis, and L. J. Stanković, "Time-frequency detection using Gabor filter bank and Viterbi based grouping algorithm," *Proc. of IEEE ICASSP*, 2005.

16. Stanković, L. J., I. Djurović, A. Ohsumi, and H. Ijima, "Instantaneous frequency estimation by using Wigner distribution and Viterbi algorithm," *Proc. of IEEE ICASSP*, 2003.

17. Djurović, I., "Viterbi algorithm for chirp-rate and instantaneous frequency estimation," *Signal Processing*, Vol. 91, No. 5, 1308–1314, May 2011.

18. Djurović, I. and L. J. Stanković, "STFT-based estimator of polynomial phase signals," *Signal Processing*, Vol. 92, No. 11, 2769–2774, Nov. 2012.

19. Djurović, I. and L. J. Stanković, "Quasi maximum likelihood estimator of polynomial phase signals," *IET Signal Processing*, Vol. 13, No. 4, 347–359, Jun. 2014.